J|A|C|S
ARTICLES
Published on Web 02/28/2006

Magneto-Optic Spectroscopy of a Protein Tetramer Binding Two Exciton-Coupled Chlorophylls

Joseph L. Hughes,*,§ Reza Razeghifard,‡ Mark Logue,‡ Aaron Oakley,§ Tom Wydrzynski,‡ and Elmars Krausz§

Contribution from the Research School of Chemistry, and Photobioenergetics, Research School of Biological Sciences, The Australian National University, Canberra, ACT 0200, Australia

Received September 25, 2005; E-mail: hughes@rsc.anu.edu.au

Abstract: In vitro chlorophyll (Chl) aggregates have often served as models for in vivo forms of long-wavelength Chl. However, the interaction of protein-bound Chl molecules is typically different than that occurring in solvent-based self-aggregates. We have chosen a water-soluble Chl-binding protein (WSCP) from cauliflower in order to help characterize the spectroscopic properties of Chl in a single well-defined native environment and also to study the pigment−pigment (exciton) interactions present in assemblies of this protein. WSCP forms tetrameric units upon binding two Chl molecules. We present the absorption, circular dichroism (CD), magnetic circular dichroism (MCD), and emission spectra at 1.7 K of recombinant WSCP tetramers containing either Chl *a* or Chl *d*. The spectroscopic characteristics provide evidence for significant exciton interaction between equivalent Chl molecules. Our simple exciton analysis allows an estimate of the molecular geometry of the dimer, which is predicted to have an "open sandwich"-type structure. We find that the ratio of the magnetic circular dichroism to absorption, $\Delta A/A$, is substantially increased (∼60%) for Chl *a* in this system compared to its value in solution. This increase is in marked contrast to substantial reductions (>50%) of $\Delta A/A$ seen in solvent-based Chl aggregates and in photosynthetic reaction centers. Current theoretical models are unable to account for such large variations in the MCD to absorption ratio for Chl. We propose that spectroscopic studies of WSCP mutants will enable a fundamental understanding of Chl−Chl and Chl−protein interactions.

Introduction

Photosystems are (bacterio)chlorophyll-containing pigment−protein complexes responsible for efficient light-induced electron transfer in photosynthesis. Properties of (bacterio)chlorophyll (B)Chl molecules important for their effective function in photosystems, such as their excitation energies or redox potentials, can be strongly influenced by their interactions with the surrounding protein environment.[1] Chl molecules bind to proteins via a number of noncovalent interactions, and the accumulated specificity of such interactions dictate the precise relative orientations and separation of Chl molecules within a photosynthetic assembly. In addition to the Chl−protein van der Waals interactions, protein residues typically provide a fifth ligand to the central metal (Mg) of Chl,[2,3] as well as giving rise to hydrogen bonding to the peripheral groups of the chlorin ring.[2] Binding is highly specific as structurally similar Chl molecules, such as Chl *a* and Chl *b*, cannot easily be interchanged. By modifying the protein site, the selective binding can be altered.[4]

The photooxidizable assembly found in the reaction center of natural photosystems is often considered to be an exciton-coupled dimer and has been the subject of extensive spectroscopic studies[5,6] to better understand its unique functionality. However, it can be a challenging task to study the optical spectroscopy of two particular Chl molecules in a photosystem that may contain up to several hundred Chl as well as other pigments. To exacerbate this problem, in general, each specific Chl-binding protein site will bind Chl molecules with different excitation energies and will exhibit an intrinsic inhomogeneous spectral broadening. This will lead to a spectrum consisting of overlapping bands that is difficult to characterize. Consequently, the study of a well-defined, isolated Chl dimer bound in a protein environment becomes appealing.

In this study, we have chosen a water-soluble Chl-binding protein (WSCP) from cauliflower, which has a very high affinity for Chl *a*.[7] This protein is capable of extracting Chl from the proteins in thylakoid membranes in aqueous suspensions, forming Chl−WSCP. The WSCP class of proteins is different from Chl-containing membrane-bound proteins. They are water-soluble, contain high β-structure content, and exhibit high

§ Research School of Chemistry.
‡ Photobioenergetics, Research School of Biological Sciences.

(1) Renger, T.; Marcus, R. A. *J. Chem. Phys.* **2002**, *116*, 9997−10019.
(2) Lutz, M.; Mäntele, W. Vibrational Spectroscopy of Chlorophylls. In *Chlorophylls*; Scheer, H., Ed.; CRC Press: Boca Raton, FL, 1991; pp 855−902.
(3) Balaban, T. S.; Fromme, P.; Holzwarth, A. R.; Krauss, N.; Prokhorenko, V. I. *Biochim. Biophys. Acta* **2002**, *1556*, 197−207.
(4) Bassi, R.; Croce, R.; Cugini, D.; Sandonà, D. *Proc. Natl. Acad. Sci. U.S.A.* **1999**, *96*, 10056−10061.
(5) Dekker, J. P.; van Grondelle, R. *Photosynth. Res.* **2000**, *63*, 195−208.
(6) Raszewski, G.; Saenger, W.; Renger, T. *Biophys. J.* **2005**, *88*, 986−998.
(7) Satoh, H.; Nakayama, K.; Okada, M. *J. Biol. Chem.* **1998**, *273*, 30568−30575.

thermal stability. Upon binding Chl, WSCP monomers oligomerize, which is a process requiring the Chl phytyl tail.[8] The ratio of bound Chl per WSCP varies depending on species. When various species are compared, this ratio has been shown to be 1, 2, or 4 per tetrameric Chl−WSCP assembly.[9] For WSCP from cauliflower that has been natively reconstituted with Chl from membrane proteins, tetrameric Chl−WSCP is the dominant oligomerized form and has been shown to contain 2 Chl.[8]

Magnetic circular dichroism (MCD) is the difference between the absorption of left and right circularly polarized light in the presence of an external magnetic field applied parallel to the absorption (transmission) direction. Electronic excitations of Chl-like molecules only exhibit MCD Faraday *B*-terms in MCD. These may have either positive or negative sign and follow the line shape[10] of the absorption feature from which they arise. The Faraday *B*-term arises from field-induced mixing of electronic states,[10] and the effect is linear in the applied magnetic field **B** when the energy separation of electronic states that are mixed is $\gg\beta\mathbf{B}$ (β is the Bohr magneton). When the *B*-term MCD for a given transition is dominated by mixing with a *single* excited state, the magnitude of the *B*-term is inversely proportional to their energy separation. Furthermore, mixing between electronic states only occurs to the extent to which transitions to these states have orthogonal polarizations. MCD becomes a particularly sensitive measure of the symmetry and angular momentum properties of the electronic states involved in optical transitions. The *B*-term MCD for the two lowest-energy electronic transitions for Chl-like molecules (Q_y and Q_x) is dominated by the field-induced mixing between these states. It is generally considered that other excitations are sufficiently removed in energy to render their contribution negligible;[11,12] however, in this work, we briefly discuss the effect that the $Q_y(1,0)$ transitions may have.

MCD is a useful tool to investigate the influence that specific local interactions have on optical transitions. Recently, MCD has been used to study[13,14] the Q_x transition and coordination state of the central Mg for Chl-like molecules, where the assignment of the Q_x transition for Chl *a* was different than that traditionally accepted.[11,15−17] Chl aggregation in solution has been phenomenologically associated with a significant reduction (≥50%) in the magnitude of MCD relative to absorption.[13,18,19] Such a reduction has also been observed in photosynthetic protein complexes containing (B)Chl[20−22] and associated with pigments in photosynthetic reaction centers where highly efficient photoexcited charge separation takes place. To our knowledge, the only theoretical treatment of the MCD of exciton-coupled systems involves incorporation of environmental effects via adjustable parameters in the simple exciton formalism[11] and treatment of angular momentum effects associated with simple exciton coupling.[12] Neither process can adequately describe large variations in the Chl *B*/*D* ratio.

In vitro (B)Chl can form self-aggregated assemblies, which have been studied in detail for over four decades by an extensive range of spectroscopic techniques, including, for example, infrared,[2,23−25] visible,[11,15,24−34] circular dichroism,[16,18,26,27,30−34] magnetic circular dichroism,[11,13,14,16,18,19] resonance Raman,[2,31,35,36] NMR,[2,25,32,34,37−39] and X-ray crystallography of Chl derivatives.[40,41] Chl derivatives have also been employed to study aggregation phenomena of (B)Chl systems,[32,33,42] and the importance of the phytyl tail in Chl self-aggregation has recently been recognized.[32,34,42] The degree of aggregation depends[15,23,25,28,29,37,43−45] on the solvent system, Chl concentration, and temperature, where it can vary from dimers, such as in dry CCl_4, to the larger oligomers of solid-state hydrated Chl *a* aggregates, for example.

The mode of Chl *a* aggregation involves[2,23−25,28,29,37,39,41,45−47] interaction between the central Mg of one Chl *a* and the 13^1, 13^3, and 17^3 carbonyl groups of a neighboring Chl *a* (IUPAC−

(8) Schmidt, K.; Fufezan, C.; Krieger-Liszkay, A.; Satoh, H.; Paulsen, H. *Biochemistry* **2003**, *42*, 7427−7433.
(9) Satoh, H.; Uchida, A.; Nakayama, K.; Okada, M. *Plant Cell Physiol.* **2001**, *42*, 906−911.
(10) Piepho, S. B.; Schatz, P. N. *Group Theory in Spectroscopy with Applications to Magnetic Circular Dichroism*. Wiley-Interscience: New York, Chichester, Brisbane, Toronto, Singapore, 1983.
(11) Zevenhuijzen, D.; Zandstra, P. J. *Biophys. Chem.* **1984**, *19*, 121−129.
(12) Hughes, J. L.; Pace, R. J.; Krausz, E. *Chem. Phys. Lett.* **2004**, *385*, 116−121.
(13) Umetsu, M.; Wang, Z.-Y.; Yoza, K.; Kobayashi, M. *Biochim. Biophys. Acta* **2000**, *1457*, 106−117.
(14) Umetsu, M.; Wang, Z.-Y.; Kobayashi, M.; Nozawa, T. *Biochim. Biophys. Acta* **1999**, *1410*, 19−31.
(15) Shipman, L. L.; Cotton, T. M.; Norris, J. R.; Katz, J. J. *J. Am. Chem. Soc.* **1976**, *98*, 8222−8230.
(16) Houssier, C.; Sauer, K. *J. Am. Chem. Soc.* **1970**, *92*, 779−791.
(17) Evans, T. A.; Katz, J. J. *Biochim. Biophys. Acta* **1975**, *396*, 414−426.
(18) Umetsu, M.; Seki, R.; Wang, Z.-Y.; Kumagai, I.; Nozawa, T. *J. Phys. Chem. B* **2002**, *106*, 3987−3995.
(19) Kobayashi, M.; Wang, Z. Y.; Yoza, K.; Umetsu, M.; Konami, H.; Mimuro, M.; Nozawa, T. *Spectrochim. Acta, Part A* **1996**, *51*, 585−598.
(20) Mimuro, M.; Kobayashi, M.; Shimada, K.; Uezono, K.; Nozawa, T. *Biochemistry* **2000**, *39*, 4020−4027.
(21) Nozawa, T.; Kobayashi, M.; Wang, Z. Y.; Itoh, S.; Iwaki, M.; Mimuro, M.; Satoh, K. *Spectrochim. Acta* **1995**, *51A*, 125−134.
(22) Smith, P. J.; Peterson, S.; Masters, V. M.; Wydrzynski, T.; Styring, S.; Krausz, E.; Pace, R. J. *Biochemistry* **2002**, *41*, 1981−1989.
(23) Ballschmiter, K.; Katz, J. J. *J. Am. Chem. Soc.* **1969**, *91*, 2661−2677.
(24) Cotton, T. M.; Loach, P. A.; Katz, J. J.; Ballschmiter, K. *Photochem. Photobiol.* **1978**, *27*, 735−749.
(25) Katz, J. J.; Shipman, L. L.; Cotton, T. M.; Janson, T. R. Chlorophyll Aggregation: Coordination Interactions in Chlorophyll Monomers, Dimers, and Oligomers. In *The Porphyrins, Physical Chemistry, Part C*; Dolphin, D., Ed.; Academic Press: New York, San Francisco, London, 1978; Vol. V, pp 401−458.
(26) Scherz, A.; Parson, W. W. *Biochim. Biophys. Acta* **1984**, *766*, 653−665.
(27) Scherz, A.; Rosenbach-Belkin, V. *Proc. Natl. Acad. Sci. U.S.A.* **1989**, *86*, 1505−1509.
(28) Scherz, A.; Rosenbach-Belkin, V.; Fisher, J. R. E. Chlorophyll Aggregates in Aqueous Solutions. In *Chlorophylls*; Scheer, H., Ed.; CRC Press: Boca Raton, FL, 1991; pp 238−239.
(29) Katz, J. J.; Bowman, M. K.; Michalski, T. J.; Worcester, D. L. Chlorophyll Aggregation: Chlorophyll−Water Micelles as Models for in vivo Long-Wavelength Chlorophyll. In *Chlorophylls*; Scheer, H., Ed.; CRC Press: Boca Raton, FL, 1991; pp 211−235.
(30) Rosenbach-Belkin, V.; Scherz, A.; Michalski, T. J.; Schiffer, M.; Norris, J. *Photochem. Photobiol.* **1994**, *59*, 579−583.
(31) Oba, T.; Watanabe, T.; Mimuro, M.; Kobayashi, M.; Yoshida, S. *Photochem. Photobiol.* **1996**, *63*, 639−648.
(32) Hartwich, G.; Fiedor, L.; Simonin, I.; Cmiel, E.; Schafer, W.; Noy, D.; Scherz, A.; Scheer, H. *J. Am. Chem. Soc.* **1998**, *120*, 3675−3683.
(33) Agostiano, A.; Catucci, L.; Colafemmina, G.; Scheer, H. *J. Phys. Chem. B* **2002**, *106*, 1446−1454.
(34) Agostiano, A.; Cosma, P.; Trotta, M.; Monsu-Scolaro, L.; Micali, N. *J. Phys. Chem. B* **2002**, *106*, 12820−12829.
(35) Cotton, T. M.; Duyne, R. P. V. *J. Am. Chem. Soc.* **1981**, *103*, 6020−6026.
(36) Callahan, P. M.; Cotton, T. M. *J. Am. Chem. Soc.* **1987**, *109*, 7001−7007.
(37) Abraham, R. J.; Rowan, A. E. Nuclear Magnetic Resonance Spectroscopy of Chlorophyll. In *Chlorophylls*; Scheer, H., Ed.; CRC Press: Boca Raton, FL, 1991; pp 797−834.
(38) van Rossum, B.-J.; Boender, G. J.; Mulder, F. M.; Raap, J.; Balaban, T. S.; Holzwarth, A.; Schaffner, K.; Prytulla, S.; Oschkinat, H.; de Groot, H. J. M. *Spectrochim. Acta, Part A* **1998**, *54*, 1167−1176.
(39) van Rossum, B. J.; Schulten, E. A. M.; Raap, J.; Oschkinat, H.; de Groot, H. J. M. *J. Magn. Reson.* **2002**, *155*, 1−14.
(40) Strouse, C. E. *Proc. Natl. Acad. Sci. U.S.A.* **1974**, *71*, 325−328.
(41) Chow, H.-C.; Serlin, R.; Strouse, C. E. *J. Am. Chem. Soc.* **1975**, *97*, 7230−7237.
(42) Fiedor, L.; Stasiek, M.; Mysliwa-Kurdziel, B.; Strzalka, K. *Photosynth. Res.* **2003**, *78*, 47−57.
(43) Ballschmiter, K.; Cotton, T. M.; Strain, H. H.; Katz, J. J. *Biochim. Biophys. Acta* **1969**, *180*, 347−359.
(44) Ballschmiter, K.; Katz, J. J. *Biochim. Biophys. Acta* **1972**, *256*, 307−327.
(45) Abraham, R. J.; Goff, D. A.; Smith, K. M. *J. Chem. Soc., Perkin Trans. 1* **1988**, 2443−2451.
(46) Shipman, L. L.; Janson, T. R.; Ray, G. J.; Katz, J. J. *Proc. Natl. Acad. Sci. U.S.A.* **1975**, *72*, 2873−2876.
(47) Moss, G. P. *Eur. J. Biochem.* **1988**, *178*, 277−328.

IUB nomenclature[47]). This interaction is typically bridged by a nucleophilic molecule(s), such as water, that is able to both ligate to the Mg and hydrogen bond to the carbonyl groups. The details of the aggregation interaction and relative Chl orientations appear to be different in the solid state of Chl−water aggregates[37,39,45,48] than for Chl dimers in solution.[2,23−25,28,29,37,43,44] In the *absence* of extraneous nucleophiles able to coordinate to the Mg, Chl *a* aggregation may occur via direct interaction of the 13^1 carbonyl group with the Mg of a neighboring Chl *a*.[2,23−25,28,29,37]

Self-aggregated (B)Chl systems have often served as models for in vivo (B)Chl.[26−29,39] However, unlike (B)Chl in solution, (B)Chl bound to a protein does not usually undergo its typical self-aggregation interactions,[2] although an exception is the light-harvesting antenna chlorosome found in green photosynthetic bacteria.[49] The carbonyl groups are often involved in hydrogen-bonding interactions with the protein,[2] and the central Mg is usually coordinated by the protein.[2,3] Each Chl molecule is locked in a specific protein-binding site established via its interaction with protein residues. An exciton coupling interaction can still occur when neighboring Chl molecules have comparable excitation energies and are also sufficiently close. This is the case for the holo-WSCP protein.

WSCP has a distinct advantage over other proteins binding one or two Chl molecules, such as the cytochrome b_6f complex (cytb_6f)[50] and the peridinin Chl protein (PCP),[51] as there are no other bound chromophores that contribute to the visible spectra. PCP is a trimer in which each monomer consists of two α-helical domains. The pigments are organized into two clusters, each containing one Chl and four peridinin molecules and are positioned in the hydrophobic space between the domains.[52] The distance between the Chl molecules of the two clusters is 17.4 Å. The cytb_6f complex, which is involved in electron transfer, contains several hemes and a β-carotene.[53] Another advantage of Chl-WSCP is that it provides a unique opportunity to study the interaction between two nominally isoenergetic and well-defined protein-bound Chl molecules.

Methods

Chl−WSCP Complex Preparation. Five milliliters of ∼30 μM WSCP in 50 mM Tris (pH 8.0) and 100 mM NaCl was first incubated for 20 min on a rotatory shaker with 0.4 mL of thylakoid membranes isolated from *Synechocystis* PCC 6803 (Razeghifard et al.[54]) or *Acaryochloris marina* (grown in low-light)[55] to prepare Chl−WSCP complexes containing either Chl *a* or Chl *d*, respectively. Thylakoid membrane concentrations were 0.7 mg Chl/mL. The mixture was then centrifuged at 11 000 rpm for 5 min using a benchtop centrifuge to remove thylakoid membranes. The supernatant was then loaded on a column packed with 0.5 mL Q sepharose to purify the Chl−WSCP from a blue-colored contaminant. The protein was collected from the flow through and concentrated to approximately 0.5 mL using a biomax-5k filter (Millipore). In preparation for spectroscopic measurements, the WSCP samples described above were mixed with either glycerol or an ethylene glycol/glycerol (1:1) cryoprotectant to a final concentration of ∼40%, then placed in a 12 mm diameter quartz-windowed cell assembly with a path length of 550 μm. This achieved an optical density of ∼0.3−0.6 in the Chl *a*(*d*) Q_y(0,0) region. The ethylene glycol/glycerol cryoprotectant produced better quality optical glasses than straight glycerol. There was no noticeable difference of any Chl *a*(*d*) spectral features in either glass, aside from a very slight narrowing of the spectra in the ethylene glycol/glycerol cryoprotectant. Further information on the expression and purification of recombinant WSCP can be found in the Supporting Information.

(Magnetic) Circular Dichroism Spectroscopy. For spectroscopic measurements, the sample cell was fixed to the sample rod and lowered into an Oxford Instruments Spectromag SM4 cryostat containing liquid helium. Cooling from room temperature to 4 K was performed over a period of ∼2−3 min to achieve glasses with good optical quality. The liquid helium was then pumped to perform spectroscopic experiments in superfluid helium at 1.7 K. Absorption, circular dichroism (CD), and magnetic circular dichroism (MCD) spectra were recorded simultaneously on a spectrometer designed and constructed[56] in our laboratory, using a Hamamatsu R669 photomultiplier tube for detection. Alternate fields of +5 and −5 T were used for MCD measurements.

Emission Spectroscopy. For emission measurements, the absorption/CD/MCD spectrometer was operated with reverse optics, by passage of the emission through the monochromator, and the signal was detected via a Hamamatsu R943-02 photomultiplier. In this manner, emission could be measured on the *same sample* as for the absorption/CD/MCD measurements. The excitation source was a Spex 0.25 M double monochromator operating with 1 mm slit widths, passed through a 630 nm filter, mounted at the cryostat perpendicular to the transmission measurement axis. The excitation monochromator beam was expanded to a size of 0.5 cm^2 at the sample. The intensity was calibrated with a Si photodiode and determined to be 7−9 $\mu W/cm^2$ in the range of 650−700 nm. The monochromator output had a spectral full-width at half-maximum (fwhm) of 2.3 nm.

Results

Even though WSCP binds Chl *a* preferentially, purified Chl−WSCP from cauliflower[7] also contains Chl *b*. To prepare Chl−WSCP complexes with only one type of Chl, it becomes necessary to reconstitute WSCP with Chl molecules in vitro. WSCP was then expressed as a fusion protein with Trx to allow folding into its native state in *Escherichia coli*. The same strategy was used by both Satoh et al.[7] and Schmidt et al.[8] to make recombinant WSCP; however, experiments were performed using the WSCP−Trx fusion protein since WSCP could not be successfully cleaved from Trx. However, in our work, we were able to cleave WSCP from its fusion partner and purify it (see Supporting Information). It is worth noting that in the absence of Trx, when a pet16b vector was used, WSCP formed inclusion bodies in *E. coli* (data not shown and Schmidt et al.[8]). In this work, we have prepared both Chl *a*−WSCP and Chl *d*−WSCP by mixing apo-WSCP with thylakoid membranes. In both cases, the formation of the Chl−WSCP complex was spontaneous. We used *Synechocystis* thylakoid membranes to obtain Chl *a*−WSCP that was free of Chl *b*. Chl *b* can also bind to WSCP, but with a lower affinity. Native Chl−WSCP purified from cauliflower[7] contains one Chl *b* per 6 Chl *a*. For

(48) Brown, C. E.; Spencer, R. B.; Burger, V. T.; Katz, J. J. *Proc. Natl. Acad. Sci. U.S.A.* **1984**, *81*, 641−644.
(49) Balaban, T. S.; Holzwarth, A. R.; Schaffner, K.; Boender, G.-J.; de Groot, H. J. M. *Biochemistry* **1995**, *34*, 15259−15266.
(50) Peterman, E. J. G.; Wenk, S.-O.; Pullerits, T.; Palsson, L.-O.; van Grondelle, R.; Dekker, J. P.; Rogner, M.; van Amerongen, H. *Biophys. J.* **1998**, *75*, 389−398.
(51) Kleima, F. J.; Wendling, M.; Hofmann, E.; Peterman, E. J. G.; van Grondelle, R.; van Amerongen, H. *Biochemistry* **2000**, *39*, 5184−5195.
(52) Hofmann, E.; Wrench, P. M.; Sharples, F. P.; Hiller, R. G.; Welte, W.; Diederichs, K. *Science* **1996**, *272*, 1788−1791.
(53) Stroebel, D.; Choquet, Y.; Popot, J.-L.; Picot, D. *Nature* **2003**, *426*, 413−418.
(54) Razeghifard, M. R.; Kim, S.; Patzlaff, J. S.; Hutchison, R. S.; Krick, T.; Ayala, I.; Steenhuis, J. J.; Boesch, S. E.; Wheeler, R. A.; Barry, B. A. *J. Phys. Chem. B* **1999**, *103*, 9790−9800.
(55) Razeghifard, M. R.; Chen, M.; Hughes, J. L.; Freeman, J.; Krausz, E.; Wydrzynski, T. *Biochemistry* **2005**, *44*, 11178−11187.
(56) Stranger, R.; Dubicki, L.; Krausz, E. *Inorg. Chem.* **1996**, *35*, 4218−4226.

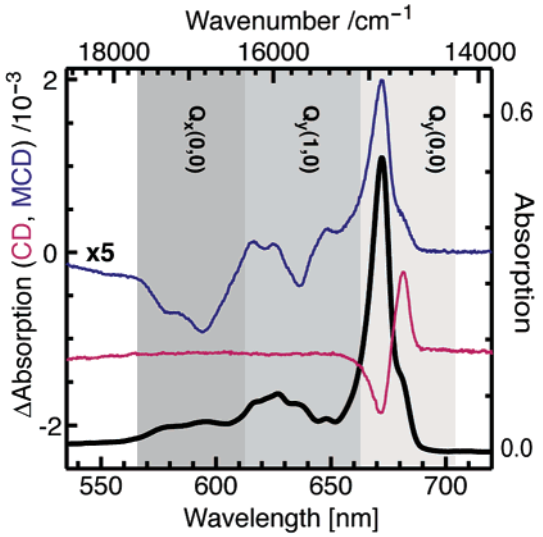

Figure 1. The absorption (black trace), circular dichroism (CD, colored bottom trace), and magnetic circular dichroism (MCD, colored top trace) of Chl *a*−WSCP at 1.7 K. The CD spectrum is offset for clarity. The MCD spectrum (per Tesla) is multiplied by a factor of 5.

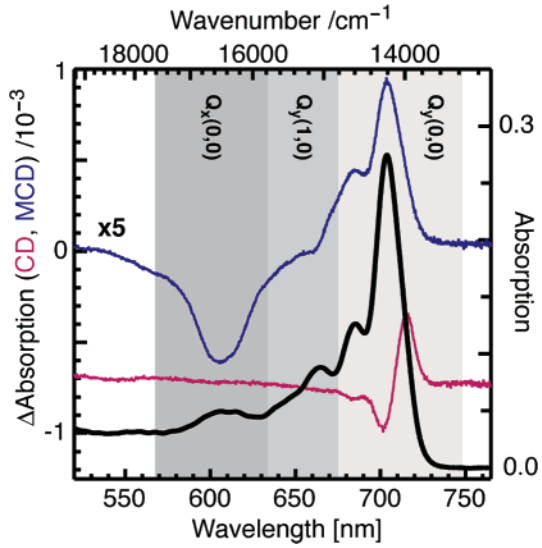

Figure 2. The absorption (black trace), CD (colored bottom trace), and MCD (colored top trace) of Chl *d*−WSCP at 1.7 K. The CD spectrum is offset for clarity. The MCD spectrum (per Tesla) is multiplied by a factor of 5. See text for discussion of the assignment of the ∼665 and ∼685 nm absorption features.

the Chl *d*−WSCP sample, thylakoid membranes extracted from *A. marina* cells grown under low light were used. The Chl *d*/Chl *a* ratio is much higher[57] when grown under low-light intensities, thus minimizing Chl *a* contamination. Also the majority of Chl *a* molecules in *A. marina* are believed to be bound to the central proteins of photosystem II complexes,[55] resulting in poor accessibility to WSCP. After binding, complexes were purified using centrifugation and ion-exchange chromatography. The Chl concentration was determined by acidifying a small volume of the Chl−WSCP complex to weaken the ligand binding of Chl to WSCP, thus removing the central Mg metal. Methanol extraction of the resulting pheophytin was then used to determine the Chl concentration of samples. A complete extraction of Chl *a* from Chl−WSCP could not be achieved by 100% methanol, ethanol, or 80% acetone.

Absorption of Chl *a*−WSCP and Chl *d*−WSCP at 1.7 K. Figure 1 shows the absorption spectrum of Chl *a*−WSCP in 40% 1:1 (v:v) ethylene glycol:glycerol. There is an absorption maximum in the $Q_y(0,0)$ region at 672.2 nm (14 877 cm^{-1}), with $\epsilon = 1.35 \times 10^5$ M^{-1} cm^{-1}. In addition, there is a clear shoulder at a longer wavelength of ∼681 nm (∼14 684 cm^{-1}). Typically, such a long-wavelength shoulder is associated with a Chl−Chl interaction, and its red shift from the main band is assigned to molecular exciton coupling of neighboring pigments.[11,15,16,25,58−60] In our case, the peak height of the absorption shoulder (Figure 1) is approximately 1/3 of the main peak. There is also a broad component at the blue edge of the $Q_y(0,0)$ absorption band (see fitting procedure below). The fwhm of the $Q_y(0,0)$ absorption band is ∼180 cm^{-1}. Such a narrow Chl *a* absorption band implies small inhomogeneous broadening, which in turn indicates a well-defined Chl *a* binding site in this protein. The fwhm of Chl in organic solvents at room temperature is typically[61] ∼400−500 cm^{-1} and relatively insensitive to temperature.[11,62] A fwhm of ∼180 cm^{-1} is narrower than that for the Chl *a* Q_y band at 4 K in PCP,[51] which binds two Chl *a* per protein monomer, and for the single Chl *a* in cytb_6f.[50] The Chl *a*−WSCP main Q_y band is red-shifted compared to that of monomeric Chl *a* in ether[19] (4 °C), PCP[51] (4 K), and cytb_6f[50] (4 K) by approximately 12, 7, and 2 nm, respectively. The $Q_y(1,0)$ vibrational envelope is clearly evident by the resolved structure in the range of ∼610−660 nm (Figure 1). The $Q_x(0,0)$ band is split into two components in our spectra, whereas only one component is particularly evident for Chl *a* in ether.[14,19]

The absorption spectrum (Figure 2) of Chl *d*−WSCP in 40% 1:1 (v:v) ethylene glycol:glycerol has a main peak in the $Q_y(0,0)$ region at 703.8 nm (14 209 cm^{-1}), with a fwhm of ∼400 cm^{-1} and peak extinction coefficient of $\epsilon = 1.16 \times 10^5$ M^{-1} cm^{-1}. The larger inhomogeneous broadening observed for Chl *d*−WSCP suggests that its binding site in the protein is not as well-defined as for Chl *a*. This is consistent with our observation that, unlike Chl *a*, Chl *d* can be readily extracted from Chl−WSCP using various organic solvents. The red shoulder that was clearly resolved in the Chl *a*−WSCP absorption spectrum (Figure 1) is less evident in the Chl *d*−WSCP spectrum (Figure 2). In addition to the main band, there are also two peaks in the Q_y region at ∼685 and ∼665 nm, which we provisionally assign to $Q_y(0,0)$ and $Q_y(1,0)$ transitions, respectively (see further discussion below). The ∼665 nm feature is possibly contamination by the impurity isochlorophyll *d*,[63] although its MCD suggests it is not $Q_y(0,0)$ (see MCD below). Lack of resolved vibrational sideband structure in the Chl *d*−WSCP spectrum is attributed to the greater inhomogeneous broadening. The Q_x

(57) Mimuro, M.; Akimoto, S.; Gotoh, T.; Yokono, M.; Akiyama, M.; Tsuchiya, T.; Miyashita, H.; Kobayashi, M.; Yamazaki, I. *FEBS Lett.* **2004**, *556*, 95−98.
(58) Scherz, A.; Parson, W. W. *Biochim. Biophys. Acta* **1984**, *766*, 666−678.
(59) Pearlstein, R. M. Theoretical Interpretation of Antenna Spectra. In *Chlorophylls*; Scheer, H., Ed.; CRC Press: Boca Raton, FL, 1991; pp 1047−1078.
(60) Shipman, L. L.; Norris, J. R.; Katz, J. J. *J. Phys. Chem.* **1976**, *80*, 877−881.
(61) Seely, G. R.; Jensen, R. G. *Spectrochim. Acta* **1965**, *21*, 1835−1845.
(62) Bellacchio, E.; Sauer, K. *J. Phys. Chem. B* **1999**, *103*, 2279−2290.
(63) Nieuwenburg, P.; Clarke, R. J.; Cai, Z.-L.; Chen, M.; Larkum, A. W. D.; Cabral, N. M.; Ghiggino, K. P.; Reimers, J. R. *Photochem. Photobiol.* **2003**, *77*, 628−637.

region of Chl *d*−WSCP (∼575−630 nm) is clearly composite of two bands. Again, they are not as well resolved as for Chl *a*−WSCP.

The dipole strength of an electronic transition can be determined by integration of the absorption spectrum[10,59,64]

$$D = 9.1834 \times 10^{-3} \int (\epsilon/\nu) \mathrm{d}\nu \quad (1)$$

where D is in units of Debye^2, ϵ is the absorption molar extinction coefficient (M^{-1} cm^{-1}), and ν is energy (cm^{-1}). We note that, in this expression, the effect of the medium is ignored.[51,6565−66] For integration of the absorption spectra, we first subtract an estimated baseline to account for absorption intensity from higher-lying states at the blue edge of the $Q_y(0,0)$ region. Failure to do this would overestimate the band area attributable to the $Q_y(0,0)$ transition, particularly for the Chl *d*−WSCP spectrum (Figure 2). We find the $Q_y(0,0)$ dipole strength for Chl *a*−WSCP is 19 ± 1 D^2. This value is very close to that for Chl *a* in ether, where no medium correction is made[16,19,65] (19−22 D^2), and for Chl *a* in PCP, where a local field correction was made[51] (17.0 ± 1.4 D^2). The integrated value for Chl *d*−WSCP is 25 ± 3 D^2. Examination of the absorption spectra (Figures 1 and 2) reveals that the Q_x transitions for both Chl *a*−WSCP and Chl *d*−WSCP are characteristically weaker, and their intensities are comparable to that for Chl molecules in ether.

Circular Dichroism of Chl *a*−WSCP and Chl *d*−WSCP at 1.7 K. CD is the difference in the absorption of left and right circularly polarized light and relates to the inherent molecular asymmetry of the chromophore. The CD spectrum of Chl *a*−WSCP (Figure 1) exhibits two oppositely signed bands, whose areas are equal in magnitude to within ±10%, that is, the spectrum is conservative to within ±10%. Oppositely signed CD bands with areas of equal magnitude can be attributed to the exciton components of a coupled molecular dimer.[16,58,59,64] Exciton coupling can induce significant CD in a system where the component monomers exhibit little or no optical activity and is due to asymmetry associated with the dimer geometry. The exciton CD is independent of the intrinsic CD of the constituent monomers. The two oppositely signed CD features (Figure 1) can be assigned to the exciton components of the coupled dimer, and the corresponding absorption bands are the main peak and long-wavelength shoulder as described above.

The peak positions of the two CD bands (671.7 and 681.6 nm) show a correspondence to the main peak and long-wavelength shoulder of the absorption spectrum. As with the absorption spectrum, there is a broad component at the blue edge of the CD spectrum (see fitting procedure below, and Supporting Information). Monomeric Chl *a* exhibits a relatively weak CD signal, with the difference extinction coefficient[16] of the Q_y band $\Delta\epsilon \sim -14$ M^{-1} cm^{-1} at room temperature in ether (fwhm ∼390 cm^{-1}). This compares (Figure 1) to $|\Delta\epsilon| \sim 170-220$ M^{-1} cm^{-1} for the Q_y CD features of Chl *a*−WSCP at 1.7 K (fwhm ∼ 150−200 cm^{-1}). Thus, the exciton CD features for Chl *a*−WSCP are almost an order of magnitude larger than the CD of monomeric Chl *a* in ether.

The CD spectrum of Chl *d*−WSCP is very similar to that of Chl *a*−WSCP, also exhibiting a derivative-type structure with a positive low-energy feature (Figure 2). The entire CD spectrum is conservative to within ±5%. The magnitude of the peak $\Delta\epsilon$ values for the derivative features are ∼100−160 M^{-1} cm^{-1}. The oppositely signed CD features peak at 701.4 and 715.6 nm and indicate the presence of two absorption bands. The lower energy CD band is positive and is associated with the red absorption shoulder (Figure 2).

There is a clearly observable negative feature at ∼685 nm in the Chl *d*−WSCP CD spectrum, whose magnitude taken from the band area (from the fitting procedure below) is ∼5 times smaller than that of the individual CD exciton components. The ∼685 nm CD feature exhibits a peak $\Delta\epsilon \sim -20$ M^{-1} cm^{-1}, which is comparable to the monomeric Chl *a* CD. This ∼685 nm feature could represent the CD of a monomeric Chl. There is also weak negative CD extending between the regions we have assigned to $Q_y(0,0)$ and $Q_x(0,0)$ of Chl *d* (Figure 2), which may be associated with the $Q_y(1,0)$ vibrational region and/or the ∼665 nm impurity[63] feature.

The rotational strength (R) is used to quantify the CD intensity in a manner analogous to the dipole strength for absorption.[59,64] For an isolated band, the rotational strength can be obtained via integration of the CD spectrum[59]

$$R = 0.247 \int \Delta\epsilon/\nu \mathrm{d}\nu \quad (2)$$

where R is the rotational strength in Debye-Bohr magneton units, $\Delta\epsilon$ is the difference absorption extinction coefficient (M^{-1} cm^{-1}), and ν is energy (cm^{-1}). By integration of the spectrum over the entire $Q_y(0,0)$ region, we determine that the net rotational strength for Chl *a*−WSCP at 1.7 K is −0.080 ± 0.004 Debye-Bohr magneton. The corresponding value for monomeric Chl *a* in ether at room temperature[16] is −0.094 Debye-Bohr magneton. Thus, it is clear that the monomeric CD of Chl *a* has not been strongly affected by the protein environment. The net rotational strength throughout the $Q_y(0,0)$ region for Chl *d*−WSCP is determined to be −0.12 ± 0.01 Debye-Bohr magneton.

Magnetic Circular Dichroism of Chl *a*−WSCP and Chl *d*−WSCP at 1.7 K. The MCD and absorption spectra of Chl *a*−WSCP can be compared in Figure 1, and in the $Q_y(0,0)$ region, the profiles agree. This is expected for Chl because its MCD is described by a *B*-term only. It has a peak $\Delta\epsilon = 96.3$ M^{-1} cm^{-1} T^{-1} at 672.2 nm. The main peak and long-wavelength shoulder seen in the Chl *a*−WSCP absorption spectrum are also observed in the MCD spectrum. There is also a negative MCD signature in the $Q_y(1,0)$ region near 636.2 nm (15 718 cm^{-1}). However, over the entire $Q_y(1,0)$ vibrational region (∼610−660 nm), the MCD band shape deviates significantly from the absorption profile. A MCD *B*-term arises from magnetically induced mixing of the nonparallel components of two or more transitions. Vibronic coupling can dramatically alter the polarization of a vibrational sideband transition build upon a $Q_y(0,0)$ electronic origin[10] from that exhibited by the origin. Therefore, it is not surprising that the MCD of Chl *a*−WSCP does not follow the absorption line shape in the $Q_y(1,0)$ region as each vibration in general exhibits a different extent of vibronic coupling.

The $Q_x(0,0)$ band of Chl *a*−WSCP can be identified in the MCD spectrum by its negative sign and approximately equal

(64) Cantor, C. R.; Schimmel, P. R. *Techniques for the Study of Biological Structure and Function, Part II*; W. H. Freeman and Company: San Francisco, CA, 1980; pp 343−846.
(65) Shipman, L. L. *Photochem. Photobiol.* **1977**, *26*, 287−292.
(66) Krawczyk, S. *Biochim. Biophys. Acta* **1989**, *976*, 140−149.

area to the $Q_y(0,0)$ band. This assignment of Q_x is different than that of Umetsu et al.[14] and is addressed further in the Discussion section. Two distinct $Q_x(0,0)$ negative MCD features near ~594 nm (16 833 cm^{-1}) and ~579 nm (17 260 cm^{-1}) are observed, consistent with the appearance of two absorption bands in the Q_x region. Their separation of ~430 cm^{-1} is far larger than what would be expected from exciton coupling of the Chl *a* Q_x transition dipoles,[12] and therefore, the origin of two Q_x features cannot readily be assigned to the interaction between nearby chromophores. Ligation of the central Mg has a more significant effect on the Chl *a* Q_x transition energies than on the Chl *a* Q_y transition energies[13−15,17,25,32] (see refs 62 and 66 for an alternative interpretation). Compared to the five-coordinated species, a pronounced red shift of several hundred cm^{-1} upon six-coordination of the central Mg is typically observed. One possibility is that the two Q_x features in Chl *a*−WSCP correspond to Chls with five- and six-coordination, respectively. However, to our knowledge, six-coordination of Chl by a protein has not been reported, and we cannot provide a definitive assignment of six-coordination for Chl−WSCP.

The MCD profile of Chl *d*−WSCP (Figure 2) matches the absorption profile from 750 to ~678 nm, consistent with the assignment to $Q_y(0,0)$ in this range. The MCD has a peak difference extinction coefficient at 703.8 nm of $\Delta\epsilon = 83.7\ M^{-1}\ cm^{-1}\ T^{-1}$. The ~665 nm feature carries a negative MCD signal that is partially obscured by the positive signal at ~685 nm. The absorption and MCD spectra at 1.7 K of Chl *d* in 4:1 (v:v) ethanol:methanol[55] exhibit a main $Q_y(0,0)$ peak at ~700 nm and complex $Q_y(1,0)$ vibrational sideband structure that has a dominantly negative MCD signature at ~670 nm. On the basis of the sign of the MCD, we can assign the peak at ~685 nm in Chl *d*−WSCP to a $Q_y(0,0)$ transition, while the ~665 nm feature may be assigned as a $Q_y(1,0)$ band. The discrepancy between the possible assignment (this work and Razeghifard et al.[55]) from the MCD of the ~665 nm feature as a vibrational $Q_y(1,0)$ band and as an impurity suggested by Nieuwenburg et al.[63] could potentially be resolved by a solvent-dependence MCD study.[14] The Q_x region (Figure 2) is again identified by its negative MCD signature and approximately equal area to the MCD in the $Q_y(0,0)$ region. The Q_x band is composite of two features, as for Chl *a*−WSCP, although they are not well resolved.

The magnitude of the MCD parameters can be determined by integration of the experimental data.[10] A spectroscopic property of interest is the ratio of ΔA (MCD) to A (absorption), $\Delta A/A$. For systems where there are nondegenerate energy levels, such as Chl, this can be reduced to a ratio of the *B*-term and the dipole strength, *B*/*D*. From Piepho and Schatz,[10] we use

$$B = (1/152.5)\int(\Delta\epsilon/\nu)\mathrm{d}\nu \qquad (3)$$

where B is in units of $Debye^2/cm^{-1}$, ν in cm^{-1}, and $\Delta\epsilon$ in units of $M^{-1}\ cm^{-1}\ T^{-1}$. Therefore, to evaluate *B*/*D* from the experimental data, we can use

$$B/D \approx 0.714\int\Delta\epsilon\mathrm{d}\nu/\int\epsilon\mathrm{d}\nu \qquad (4)$$

We obtain a value of $B/D = (6.4 \pm 0.3) \times 10^{-4}/cm^{-1}$ for Chl *a*−WSCP. This was obtained by integration of the spectra from 700 to 652 nm after subtraction of a baseline estimate to account for $Q_y(1,0)$ absorption intensity at the blue edge of the $Q_y(0,0)$ region. To estimate *B*/*D* for Chl *a* in ether, we use the data of either Kobayashi et al.[19] or Houssier and Sauer[16] and find $B/D = 3.96 \times 10^{-4}$ or $2.71 \times 10^{-4}/cm^{-1}$, respectively. Thus, the value at 1.7 K for Chl *a* bound to WSCP is ≥60% larger than that for Chl *a* in ether near room temperature. This is intriguing, given the phenomenon reported by Kobayashi and co-workers,[13,18,19] which associates the Q_y-band *B*/*D* ratio with the degree of (B)Chl aggregation. In this phenomenology, the *B*/*D* ratio is *lower* for aggregated forms than for the monomer, and reduces as 1/*n*, where there are *n* monomers in the aggregate. This behavior has been attributed to exciton coupling.[13,14,18−21] However, it has been shown that large variations in *B*/*D* for exciton-coupled Chl-like systems are not explained via simple exciton theory.[12] Our Chl−WSCP system provides the first observation of a substantial *increase* in *B*/*D* for Chl-like systems. Specific Chl−protein and/or nonexcitonic Chl−Chl interactions could provide the basis for an explanation of such *B*/*D* variations, as well as consideration of the $Q_y(1,0)$ transitions.

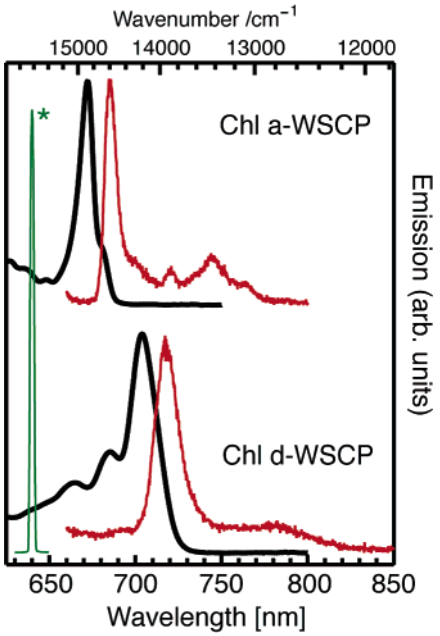

Figure 3. The emission spectra (red traces) of Chl *a*−WSCP (top panel) and Chl *d*−WSCP (bottom panel) at 1.7 K. The excitation source (∗green trace) was at 640 nm with fwhm = 2.3 nm. The corresponding absorption spectra (black traces) are presented for comparison. The emission spectra have not been corrected for the instrument response.

The *B*/*D* value for Chl *d*−WSCP is determined to be $(4.6 \pm 0.5) \times 10^{-4}/cm^{-1}$, as described above, which is similar to that for Chl *a*−WSCP. The difference (to within ~10%) in *B*/*D* values for Chl *a*−WSCP and Chl *d*−WSCP can be accounted for by the larger dipole strength of Chl *d*, if the angular momentum contribution to the *B*-term is the same for Chl *a* and Chl *d*. From the data presented in Razeghifard et al.,[55] the monomeric value of *B*/*D* for Chl *d* in 4:1 ethanol/methanol can be estimated as $(7 \pm 2) \times 10^{-4}/cm^{-1}$.

Emission of Chl *a*−WSCP and Chl *d*−WSCP at 1.7 K. Figure 3 (top panel) shows the emission spectrum of Chl *a*−WSCP at 1.7 K, as well as the absorption spectrum in the Q_y region for comparison. While there are two resolved absorption bands in the $Q_y(0,0)$ region, a single main emission band is observed peaking at 685 nm. The shift of the main emission band from the peak of the long-wavelength absorption shoulder is ~80 cm^{-1}. This shift is the same as that reported for Chl *a* in PCP.[51] For the single Chl *a* in the cytb_6f, the shift[50]

between the absorption and emission is ~165 cm^{-1}. The absence of any emission from the main absorption band precludes the possibility of nonspecifically bound Chl molecules contributing significantly to this absorption feature. This is consistent with the interpretation that both these absorption features are components of an exciton-coupled system.

For Chl *d*−WSCP, the main emission peak is at 717.4 nm (13 939 cm^{-1}) and is shifted by ~75 cm^{-1} from the low-energy absorption shoulder. No emission peak is observed from the main absorption peak (703.8 nm). We note if the Chl *d*−WSCP ~665 nm absorption feature were a Q_y(1,0) band, as suggested by the sign of its MCD (see above), we might expect a corresponding feature in the emission spectrum. The absence of such a feature in the Chl *d*−WSCP emission spectrum is understandable as the vibronic coupling of this mode to the ground state of Chl *d* will be characteristically different than its coupling to the excited state(s), thereby breaking the mirror symmetry between absorption and emission.

Discussion

Assignment of Q_x from MCD Spectra. Our assignment of the Q_x transition agrees with that traditionally made for five-coordinate Chl *a*,[11,15−17] but is different than that of Umetsu et al.,[14] who assign the region of the spectrum denoted Q_y(1,0) in our work on Chl *a*−WSCP as due to Q_x. Umetsu et al.[14] obtained MCD and absorption spectra of both five-coordinate and six-coordinate Chl *a* and performed a Gaussian fit of the visible region of their spectra. This required 7 Gaussian bands for each spectrum. They searched for a correlation between *B*/*D* and 1/Δ*E* of the bands used in their fit, where Δ*E* was the energy separation between the bands. A correlation was seen between Q_y and only one of the other Gaussian bands, which they assigned to be Q_x. The observation of fine structure in Chl *a*−WSCP spectra provides clear evidence that the region of ~610−660 nm corresponds to Q_y(1,0) transitions and that the traditional assignment of Q_x (see above) is indeed correct. The MCD observed in this region does not have the same *B*/*D* as the electronic origin, indicating that these features gain intensity via a vibronic coupling mechanism. If the features corresponded to totally symmetric modes with their intensity governed purely by Franck−Condon overlap factors between the ground and excited state in the usual way, then they would necessarily have the same polarization as the electronic origin and thus the same MCD *B*/*D*. The analysis leading to the assignment of Q_x by Umetsu et al.[14] may need to be reconsidered in light of this discussion.

Accounting for Large Variations in *B*/*D*. We now consider a number of factors that may influence the Chl *B*/*D* ratio. First, the Q_y and Q_x dipole strengths for Chl *a*−WSCP are very similar to those for Chl *a* in ether, and so any variations in *D* are unlikely to be responsible. Other factors to be considered are the energy separation between the Q_x and Q_y transitions and the angular momentum associated with exciton coupling. The MCD *B*-term for Chl is inversely proportional to the energy separation between Q_y and Q_x states. We compared the energy separation between the Q_y and Q_x bands of Chl *a*−WSCP (Figure 1) to that of ~2250 cm^{-1} for monomeric Chl *a* in ether.[16,19] This mechanism can only account for a *B*/*D* increase of up to 15%. An exciton-coupled system gives rise to an angular momentum associated with the molecular aggregate beyond that of the intrinsic monomeric components. This angular momentum is responsible for the strong CD observed with exciton-coupled molecular systems.[64] We have considered this process for an arbitrary dimer and shown[12] that the Chl MCD *B*/*D* is affected by at most a few percent. In light of our discussion regarding the effect of Q_y(1,0) transitions on the Chl *a* *B*-term MCD, we feel that theoretical investigation of the effect of electron vibrational coupling may aid our understanding of large variations in *B*/*D* for Chl systems.

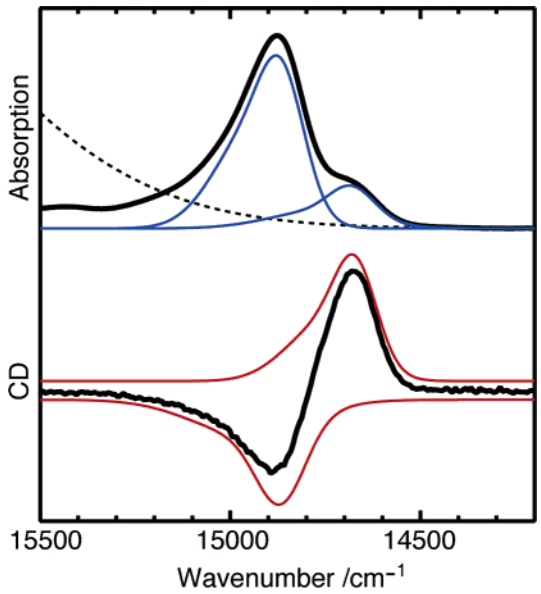

Figure 4. Fits (colored traces) composite of a sharp origin band and a broader phonon sideband of both exciton components, to the Chl *a*−WSCP absorption (black trace, top panel) and CD (black trace, bottom panel) spectra at 1.7 K. The dotted line in the top panel is a baseline estimate for the region <15 200 cm^{-1} to account for the absorption tailing from higher-lying states into the Q_y(0,0) region. The fits to the CD spectrum have been offset for clarity, and an estimate of the small monomeric contribution has been subtracted (see text and Supporting Information for details, and Table 1 for fit parameters).

Gaussian Analysis and Assignment of the Q_y(0,0) Optical Spectra. We model the optical spectra of each exciton component in the absorption and CD spectrum of Chl *a*−WSCP as an origin band plus a phonon sideband to higher energy, and our Gaussian fit is shown in Figure 4 (see Supporting Information for details). The MCD spectrum was not fit since an exciton analysis of the MCD is beyond the scope of the present work. We assume the displacement of the phonon sideband to be the same for each exciton component, and the ratio of the absorption band areas of the phonon sidebands is taken to be the same as the ratio for the origin components. Absorption and CD spectra can be well described by this model, and the resulting fit parameters for Chl *a*−WSCP are presented in Table 1. There is a significant variation in parameters obtained from absorption compared to those obtained from CD. A global fit of absorption and CD results in a visibly poorer fit. We attribute the difference in parameters for the sharper components to a noncorrelated variation in exciton coupling within the inhomogeneous distribution of dimers. Such a process is termed diagonal disorder.[51]

The intensity of the phonon sideband is determined by the electron−phonon coupling, quantified by the Huang−Rhys parameter, *S*. A large value ($S > 1$) indicates stronger coupling and greater absorption intensity in the phonon sideband, relative to the zero-phonon origin. The displacement of the phonon

Table 1. Parameters from the Gaussian Fit to the Chl *a*−WSCP Optical Spectra[a]

	band 1	band 2	phonon band 1	phonon band 2
$\bar{x}$ (cm^{-1})	14680 ± 10 (14670 ± 10)	14860 ± 10 (14870 ± 10)	14770 ± 30 (14745 ± 40)	14950 ± 30 (15015 ± 40)
fwhm (cm^{-1})	140 ± 10 (120 ± 10)	140 ± 10 (150 ± 10)	300 ± 50 (200 ± 30)	220 ± 30 (375 ± 50)
absorption band areas	0.27 ± 0.07	1.0 ± 0.3	0.33 ± 0.09	1.2 ± 0.3
CD band areas	1.0 ± 0.1	−1.0 ± 0.1	1.3 ± 0.1	−1.3 ± 0.1

[a] Fit parameters for the $Q_y(0,0)$ absorption and CD spectra of Chl *a*−WSCP. See text for details. The band areas are relative, so that they represent the ratio of band areas. The values in parentheses are for the fit to the CD spectrum. The band areas are relative, and normalized to band 2.

sideband from the sharper origin band in the fit to the absorption is 90 ± 20 cm^{-1}, indicating coupling of the Chl *a* excited state to a relatively high-frequency phonon mode of ∼90 cm^{-1}. A typical protein-bound Chl *a*[50,51] involves lower phonon frequencies of ∼20−30 cm^{-1} and electron−phonon coupling of the order $S \sim 0.3-1$. The displacement between emission and absorption of the low-energy dimer band of ∼80 cm^{-1} (see above) is consistent with such typical electron−phonon coupling to a low-frequency mode. This coupling appears in addition to coupling to the higher frequency mode established above. In light of this, our "origin band" in the fit is actually composite of the true (0,0) origin and the typical low frequency (∼20−30 cm^{-1}) phonon mode. Energy selective spectroscopic measurements, such as spectral hole burning and fluorescence line narrowing, could better characterize the phonon features in the Chl−WSCP optical spectra and allow quantification of the electron−phonon coupling strengths.

To adequately describe the $Q_y(0,0)$ absorption spectrum of monomeric Chl *a* in ether, Katz et al.[25] used two Gaussian bands, one significantly broader than the other. They suggested that this might reflect coupling of the Q_y electronic transition to one or more low-frequency vibrational modes, such as out-of-plane puckering of the entire macrocycle, or modes involving Mg. They[25] also required two sharp bands and one broad band to fit the $Q_y(0,0)$ absorption spectrum of a Chl *a* dimer in CCl_4 solvent. These observations are consistent with our approach that uses sharp and broad components to fit the Chl *a*−WSCP $Q_y(0,0)$ spectra and recent studies[67] on the in vivo and in vitro Chl *a* band shape.

We performed an analysis of the Chl *d*−WSCP $Q_y(0,0)$ absorption and CD spectra in analogy to that made for Chl *a*−WSCP. The minimum requirement to describe the Chl *d*−WSCP $Q_y(0,0)$ absorption spectrum is three Gaussian bands, two for the main band and one for the feature at ∼685 nm. The sign and magnitude of the MCD of this band is characteristic of a Chl $Q_y(0,0)$ feature. The possibility of it being a vibrational sideband of Chl *d* is also contra-indicated by the absence of any such feature in the absorption and MCD spectra of this pigment in an ethanol/methanol glass at 1.7 K.[55] The magnitude of the CD of the ∼685 nm feature is consistent with it being associated with monomeric Chl rather than an exciton-coupled dimer. Since this protein preferentially binds Chl *a*, we suggest that this ∼685 nm Chl *d* absorption may be associated with a fraction of the WSCP lacking a native tetrameric structure.

Table 2. Molecular Quantities Determined from the Optical Spectra[a]

	D (Debye^2)	$BlD \times 10^4$ ($/cm^{-1}$)	J (cm^{-1})	θ_{12}^+ (deg)	θ_{12}^- (deg)	$\lvert R_\pm \rvert$ (D-β)
Chl *a*−WSCP	19 ± 1	6.4 ± 0.3	90 ± 20	60 ± 15	120 ± 15	0.8 ± 0.1
Chl *d*−WSCP	25 ± 3	4.6 ± 0.5	130 ± 25	70 ± 20	110 ± 20	0.6 ± 0.1

[a] The Q_y transition dipole strength D, angle between Q_y transition dipole moments $\theta_{12}^\pm$, exciton coupling energy J, and the magnitude of the rotational strength $|R_\pm|$ (in Debye-Bohr magneton units) determined from the absorption and CD spectra for Chl *a*−WSCP and Chl *d*−WSCP. See text for further details.

Unlike Chl *a*−WSCP, in a minimal description, the main $Q_y(0,0)$ band for Chl *d*−WSCP does not require sharp (origin) and broad (phonon) components to fit the spectrum satisfactorily. This is due to the increased line widths in the Chl *d*−WSCP spectra. The two features that are fit to the main band are assigned to the exciton components of a coupled Chl *d* dimer, as for Chl *a*−WSCP. Additional Gaussian components were required to fit the CD spectrum to account for the ∼685 nm feature and the weak intensity throughout the $Q_y(1,0)$ region. For the two dimer components in the fit, the ratio of the absorption band areas and the exciton rotational strength were very similar to those for Chl *a*−WSCP (Table 2), while the energy separation was slightly larger, which in the transition-dipole−transition-dipole coupling model is consistent with the greater dipole strength of Chl *d*.

Finally, we note that our Gaussian analysis provides a minimal description of the optical spectra and Chl absorption band shapes, but nevertheless describes the general phenomenology. More realistic representation of Chl *a* absorption band shapes can be made that explicitly account for vibrational/vibronic structure.[1,67,68] More extended versions of exciton theory may consider a larger number of interactions (e.g., inter-dimer), nonresonant interactions,[58,59] diagonal disorder,[51] charge-transfer character,[59] environmental[11] or local-field[51] effects, and electron-vibrational coupling,[1,68,69] for example. With respect to the latter, we emphasize that our assumption of equal mean phonon frequencies for all exciton states is a significant simplification. With further structural and spectroscopic studies on Chl−WSCP, the application of more advanced exciton formalism to the Chl *a*−WSCP system will yield more detailed information regarding the Chl−Chl and Chl−protein interactions.

Dimer Geometry from an Analysis of the Optical Spectra. We can use the data obtained from the fit to the optical spectra to provide an estimate of the relative orientation of the Q_y transition dipole moments of each Chl *a* in the dimer. Assuming the orientations of the transition dipole moments are molecule fixed, the basic geometry of the dimer can be estimated in the absence of high-resolution crystal structure data, and we have used simple exciton theory for this purpose. We limit our discussion here to Chl *a* because the exciton analysis for the Chl *d*−WSCP spectra was analogous to that for Chl *a*−WSCP, and the results were very similar. Details of the analysis are provided in Supporting Information. We stress that a detailed interpretation of the Chl *a*−WSCP structure should only be made with the advent of structural X-ray spectroscopic data, and that our analysis provides an estimate of the relative orientation of the molecular planes.

(67) Zucchelli, G.; Jennings, R. C.; Garlaschi, F. M.; Cinque, G.; Bassi, R.; Cremonesi, O. *Biophys. J.* **2002**, *82*, 378−390.
(68) Renger, T. *Phys. Rev. Lett.* **2004**, *93*, 188101−188104.
(69) Kuehn, O.; Renger, T.; May, V. *Chem. Phys.* **1996**, *204*, 99−114.

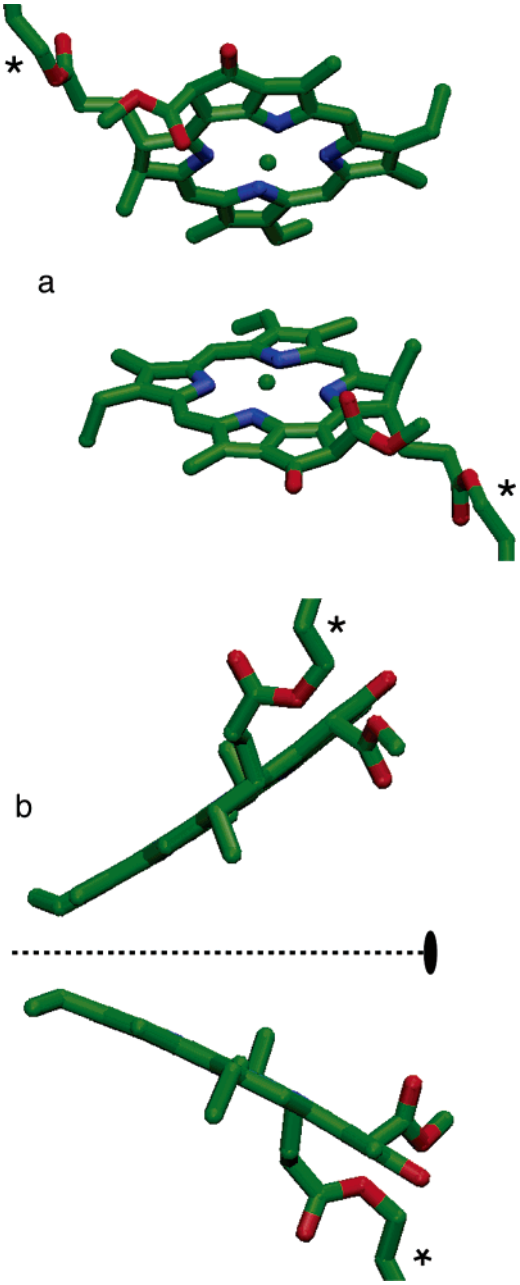

Figure 5. Our estimated geometry for the Chl *a* dimer of Chl *a*−WSCP. The views are parallel (a) and orthogonal (b) to the 2-fold axis relating the Chl *a* molecules. The dotted line and oval represent to 2-fold axis in (b). The view in (a) is from the open end of the sandwich dimer. The phytyl tails have been truncated (∗) for clarity.

Figure 5 shows our estimate of the molecular geometry of the Chl *a* dimer in Chl *a*−WSCP, viewed both parallel to the 2-fold axis (Figure 5a) and orthogonal to it (Figure 5b). It has an "open sandwich"-type structure, with the Chl *a* molecular planes skewed with respect to both each other and the 2-fold axis. In Figure 5, the Mg−Mg separation is 7.6 Å and the face-to-face separation of the Chl *a* molecular planes is 4.0 and 13.7 Å at the "closed" and "open" ends of the dimer, respectively. The hydrophobic phytyl tails have been truncated in Figure 5 (*) for clarity and are toward the open end of the dimer. Given that the phytyl tails are required for oligomerization of WSCP,[8] their spatial separation in our estimated structure is consistent with a phytyl−protein interaction, and not phytyl−phytyl interactions, as for some self-aggregates.[34] A phytyl−solvent interaction, which is possibly important for Chl self-aggregation in solvents,[42] is also unlikely given that our studies are on a natively folded water-soluble protein.

Our estimate of the dimer geometry places the 13^1, 13^3, and 17^3 carbonyl groups at the open end of the sandwich structure. This is consistent with the engagement of these peripheral groups, particularly the 13^1 carbonyl, in hydrogen bonding to the protein and not self-aggregation interactions. If self-aggregation interactions were important, we might expect a closer relationship between the carbonyl groups of one Chl *a* and the Mg of the other (see Introduction). We can only speculate on the occupancy of the interior of the open sandwich structure. Some possibilities may be that it is largely vacant, occupied by protein, perhaps involves a hydrogen-bonding network of water molecules coordinated to the Mg and carbonyl groups, or some combination of these.

Conclusions

We have presented a characterization of the optical spectroscopy of recombinant WSCP from cauliflower containing either Chl *a* or Chl *d*.

(i) Features in the optical spectra were shown to arise from an exciton-coupled dimer of Chl molecules, consistent with the known property of WSCP in forming a tetramer upon binding two Chl molecules.

(ii) An estimate of the dimer geometry was made based on a simple exciton analysis of the optical spectra and found to exhibit an open sandwich-type phenomenology of the chlorin rings. We suggest that the Chl planes are oriented with the phytyl tails as well as the 13^1 and 13^3 carbonyl groups toward the open end of the dimer sandwich.

(iii) The emission spectra establish that essentially all Chl bound to WSCP are connected via energy transfer.

(iv) The electronic Chl *a* states couple to two distinct phonon systems, one of which is typical for Chl *a*, and the other is a relatively high-frequency phonon mode of the order ∼90 cm^{-1}. The data are consistent with a relatively low electron−phonon coupling strength, typical for Chl *a* ($S \sim 0.3-1$).

(v) The first characterization of the MCD of Chl bound to a single protein environment was made. The diagnostic *B*/*D* value for Chl *a* in WSCP was found to be at least 60% larger than that for monomeric Chl *a* in ether. By contrast, there is a 50% or greater *reduction* in *B*/*D* for other solvent-based Chl aggregates and ∼50% reductions for photoactive Chl assemblies in natural photosystems.

The Chl−WSCP system presents an exceptional opportunity to determine the detailed nature of Chl−protein and Chl−Chl interactions. When the potential information available from mutagenesis is combined with parallel spectroscopic and theoretical studies, a number of important and fundamental issues can be directly addressed in a minimal system. Factors influencing the Chl binding affinity, excitation energy, homogeneous broadening, and electron−phonon coupling can be determined as well as the large variations seen in the MCD *B*/*D* value.

Acknowledgment. This work was supported in part by Australian Research Council Discovery Grant (DP0450421).

Supporting Information Available: Expression and purification of recombinant WSCP; details of simple exciton analysis for WSCP; further details of Gaussian analysis of absorption and CD spectra; further details of the estimation of molecular geometry for Chl *a* dimer of WSCP. This material is available free of charge via the Internet at http://pubs.acs.org.

JA056576B